

Calculations of Near-Fields of ICRF Antenna for ASDEX Upgrade

Vl. Bobkov, F. Braun¹, J.-M. Noterdaeme^{1,2} and ASDEX Upgrade team¹

¹Max-Planck-Institut für Plasmaphysik, EURATOM-Association, Garching, Germany

²Ghent University, EESA Department, Gent, Belgium

Introduction

Impurity sputtering at ICRF (Ion Cyclotron Range of Frequencies) antennas and structures connected along magnetic field lines to the antennas can be a problem in today's high-Z first wall material fusion experiments [1,2] and is a concern for future fusion reactors. For ASDEX Upgrade, an improved antenna design is needed to minimize tungsten (W) source during ICRF operation that is due to elevated sheath voltages on the field lines connected to ICRF antennas.

According to [3], sheath voltage is defined by a parallel voltage $V_{\parallel} = \int E_{\parallel} \cdot dl$ along magnetic field lines in front of an antenna. The High Frequency Structure Simulator (HFSS) Code [4] is capable to calculate E_{\parallel} for relatively complicated 3D geometry, though only with a simple model of the plasma (water). Nevertheless, the characteristic properties of the near-fields are consistent with other codes with a better plasma model, such as ICANT [5] and TOPICA [6]. The advantage of HFSS code is that it is fast for high resolution and can be currently run on a single high-end workstation.

The recent measurements at ASDEX Upgrade (AUG) ICRF antennas agree reasonably well with HFSS calculations [7]. This strengthens the confidence in the use of HFSS calculations to develop an improved antenna with reduced E_{\parallel} fields for AUG which would lead to a lower W source during ICRF operation.

Description of calculations

A planar model of an antenna is placed in a square cuboid (2.27 m × 1.5 m × 0.6 m) with radiation conditions as boundaries. In the cuboid, a water tank (2.27 m × 1.5 m × 0.3 m) is placed 4 cm in front of the antenna. The output of the HFSS code consists of arrays of real and imaginary parts of the x, y, z components of electric fields $E_{x,y,z}$ at the antenna front plane with 2.27 m × 1.5 m dimensions. The plane is 1 cm in front of the antenna Faraday Screen (FS). At this plane, $E_{x,y,z}$ are calculated for 1 W forward power put into each of coaxial inputs. The fields are then re-normalized to 1 MW net power using the s_{11} parameter of the left antenna strap. Due to relatively small cross-coupling between antenna straps, the error due to such normalization is usually below 5 %. The parallel fields E_{\parallel} are calculated for magnetic field inclination angle of 0° or 11°. The parallel voltages V_{\parallel} are calculated as $V_{\parallel} = \int E_{\parallel} \cdot dl$ on the magnetic field lines passing in front of the antenna at the noted inclination angles. As an additional figure of merit of parallel voltages for many possible magnetic field line geometries which may start and/or end on many antenna structures, the integral of *absolute* values $V_{abs} = \int |E_{\parallel}| \cdot dl$ is calculated and used for comparison between antenna concepts.

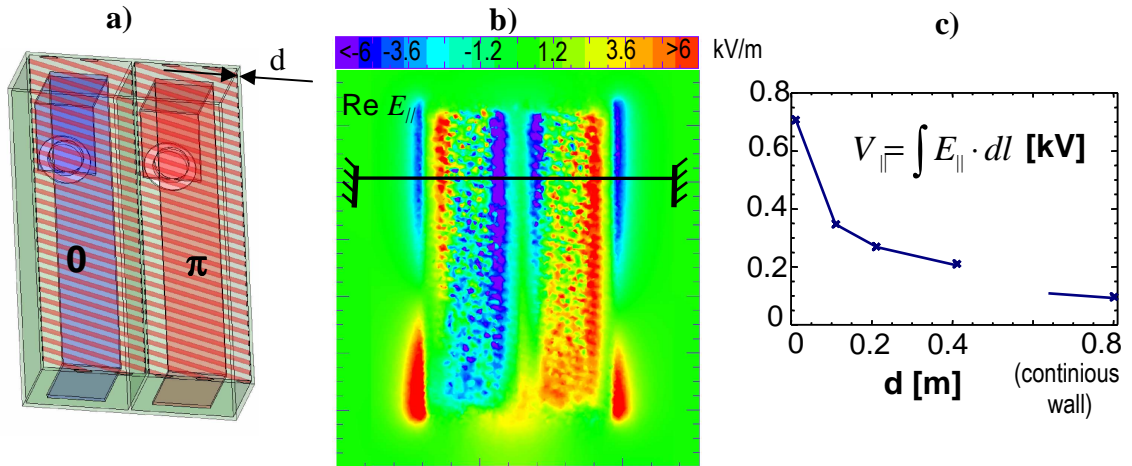


Fig.1. a) Model for a simple 2-strap antenna ($d=0.01$ m). b) Contour-plot of Re part of $E_{||}$ at 0° magnetic field inclination angle, $P_{RF}=1$ MW. c) Dependence of $V_{||}$ on the field line from (b) on antenna side wall thickness d .

Results and discussion

In Fig.1a, a model of a simple antenna with two symmetrical straps and 15° inclined FS is presented. As seen in Fig.1b, which shows a contour plot of real part of the antenna $E_{||}$ at 0° inclination angle, there are high fields in the antenna corners. These fields are strongly influenced by the antenna box which carries image currents of the antenna straps on various paths of the antenna box. The parallel fields $E_{||}$ appear on the outer walls. Here, the electric fields are forced to be perpendicular to the box surfaces and get a large parallel component at the edge of the antenna outer walls. One can generalize, that $E_{||}$ are strongly influenced by the image currents on various structures of the antenna box, and appear at the locations where the surface intersects magnetic field lines.

To reduce $V_{||}$ in front of the antenna, it is necessary to reduce $E_{||}$ fields on the box. One of the main parameters which influence $E_{||}$ fields is the thickness d of the antenna side wall (see Fig.1a) which represents a simple model for antenna limiter. Fig.1c presents $V_{||}$ calculated on the horizontal field line shown in Fig.1b versus d . When d is increased, the distance between the outer wall and the antenna straps is increased, i.e. the distance is increased between the surface which intersects magnetic field lines and the locations where high image currents and high electric fields exist. This decreases $E_{||}$ fields on the outer wall. Thus the box contribution, dominant with small d , fades away when d is increased. It does not exist at all when d reaches 0.8 m which is the distance where the outer wall coincides with the radiation condition at the edge of the calculation cuboid. This case corresponds to an antenna embedded in a continuous infinite wall which does not intersect magnetic field lines. In this case the relatively small value of $V_{||}$ originates solely from the contribution of antenna straps. This contribution is non-zero due to an asymmetry introduced by the 15° inclined FS.

Figure 2a presents a model for the original AUG antenna. As one observes, the limiters are the locations where $E_{||}$ mostly appear. As was described above, the reasons for this are significant image currents, high electric fields at the antenna and intersection of the limiter curvature with magnetic field lines. Depending on the alignment of the limiter curvature with respect to the magnetic field lines, either positive or negative $E_{||}$ fields appear on the limiter sides.

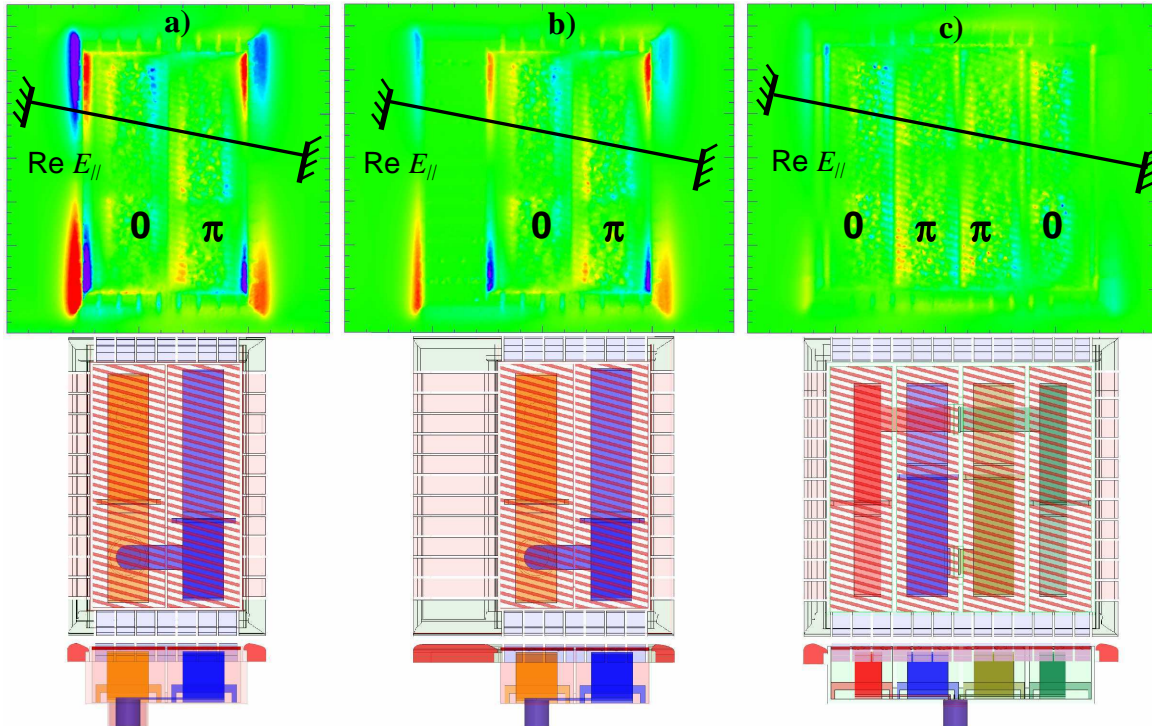


Fig.2. Contour plots for $Re(E_{||})$ at 11° inclination angle at $P_{RF}=1$ MW (same scale as Fig.1b) and antenna designs: a) original AUG antenna; b) possible AUG antenna with a broad limiter; c) possible 4-strap AUG antenna.

For the *original* AUG antenna, it is not possible to integrate the box in a continuous wall and avoid the $E_{||}$ fields due to the box contribution. A limited space exists only at one side of the antenna. This allows broadening of one limiter only, as seen in Fig.2b. However a reduction of $E_{||}$ appears to be already quite effective. This can be seen in Fig. 3 which shows $V_{||}$ on field lines passing in front of antenna and in Fig. 4 which shows V_{abs} for original AUG antenna (introduced in Fig.2.a) as red dotted curves and for broad AUG antenna (introduced in Fig.2.b) as blue dashed curves. The voltages are plotted versus the vertical position Z along the middle septum of the antenna model.

In order to reduce $V_{||}$ not only on the field lines passing an antenna, but also on other field lines, for example starting on one of the antenna limiters, it is necessary to reduce V_{abs} . This parameter shows the overall reduction of $E_{||}$ fields.

With an antenna which has more than 2 straps, it is possible to reduce $E_{||}$ further, in particular the contribution from antenna outer walls. For such antenna it is advantageous to phase the inside-straps out-of-phase with respect to the outer-straps, i.e. with $(0\pi\pi0)$ phasing. Fig. 2c shows one possible concept of a 4-strap antenna for AUG. One observes a significant reduction of $E_{||}$ fields at the side walls. This happens due to a relatively large contribution of the inside-straps which counteract the image

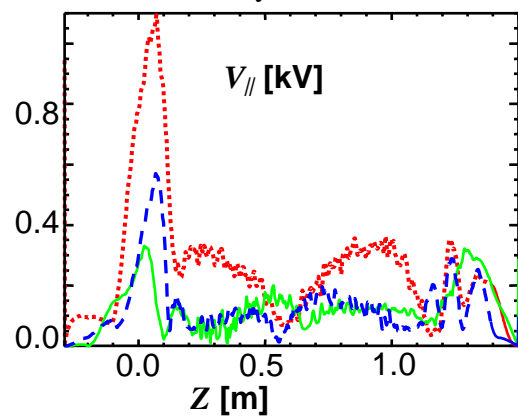


Fig.3. $V_{||}$ for original AUG antenna (red dotted), antenna with a broad limiter (blue dashed), 4-strap AUG antenna (green solid).

currents and electrical fields of the outer-straps. For an effective reduction, the inside-straps should deliver more power than the outer-straps. This can be done either by feeding the inside- and the outer- straps differentially, or as is shown for the antenna design in Fig. 2c, by shortening the width of the outer-straps. In this case $E_{||}$ fields do not originate mostly from a few specific locations like the limiters at the antenna outer walls, but originate rather from the whole antenna. While the reduction is not observed for the field lines passing in front of the antenna (Fig.3 green), a significant reduction is observed for V_{abs} (Fig.3 green) which is a measure of $V_{||}$ for various magnetic field line geometries.

Further optimizations of the 4-strap antenna should include a reduction of the internal antenna strap $E_{||}$ fields by the use of a more optically closed FS. The shortening of the antenna straps also leads to a better $E_{||}$ distribution. In both cases there is a trade-off between a smaller $E_{||}$ (or a better $E_{||}$ distribution) and a better coupling. To reduce connection lengths of magnetic field lines, one should implement a limiter between the inside-straps.

Conclusions

Simple 2-strap, present AUG antennas and options for AUG antennas with reduced $E_{||}$ fields were modelled using HFSS code in order to make a basis for AUG ICRF antenna design with minimized impurity source during operation. The calculations show that high $E_{||}$ fields are located where antenna box intersects magnetic field lines. These $E_{||}$ fields can be reduced by putting the locations of the intersection further away from the antenna, where the effect of the image currents and electric fields of the antenna is lower. For AUG antenna, this broadening of antenna limiters can in practice only be done on one antenna side. Nevertheless this reduces $E_{||}$ noticeably. A further significant reduction of such $E_{||}$ fields can be achieved for 4-strap antenna operating in $(0\pi\pi0)$ phasing, with more power applied to the inside-straps than to the outer-straps, or the outer-straps with shorter width. Further optimizations will exploit: 1) reduction of $E_{||}$ attributed to internal antenna fields by using a more closed Faraday screen; 2) optimization of $E_{||}$ distribution by shortening antenna strap length; 3) shortening field line connection lengths by introducing a poloidal limiter at the antenna middle.

References

- [1] R Dux et al., Journal of Nuclear Materials **363-365** (2007) 112.
- [2] S. Wukitch et al., Journal of Nuclear Materials **363-365** (2007) 491.
- [3] Perkins F., Nucl. Fusion **29** 4 (1989), 583.
- [4] High Frequency Structure Simulator (HFSS), www.ansoft.com.
- [5] L. Colas, S. Heurax, S. Brémond, G. Bosia, Nucl. Fusion **45** (2005) 767.
- [6] V. Lancellotti et al., Nucl. Fusion **46** (2006) S476.
- [7] V.I. Bobkov, submitted to Journal of Nuclear Materials, PSI-18 Conference.

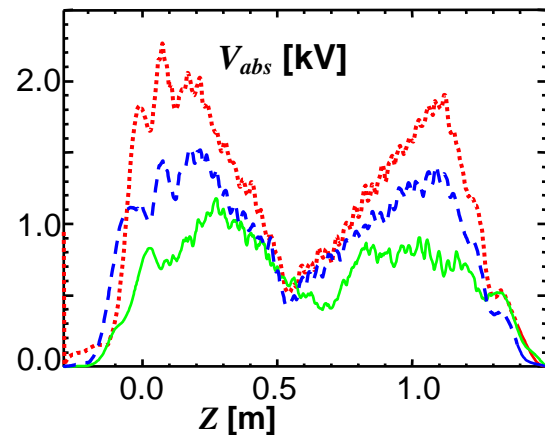


Fig.4. V_{abs} for original AUG antenna (red dotted), antenna with a broad limiter (blue dashed), 4-strap AUG antenna (green solid).